# Radiosynthesis and In Vivo Evaluation of Novel Radioligands for PET Imaging of Cerebral 5-$HT_7$ Receptors

Hanne D. Hansen[1,2], Matthias M. Herth[1–4], Anders Ettrup[1,2], Valdemar L. Andersen[1–4], Szabolcs Lehel[3], Agnete Dyssegaard[1,2], Jesper L. Kristensen[3], and Gitte M. Knudsen[1,2]

*[1]Center for Integrated Molecular Brain Imaging, Copenhagen University Hospital Rigshospitalet, Copenhagen, Denmark; [2]Neurobiology Research Unit, Rigshospitalet and University of Copenhagen, Copenhagen, Denmark; [3]Department of Drug Design and Pharmacology, Faculty of Health and Medical Sciences, University of Copenhagen, Copenhagen, Denmark; and [4]PET and Cyclotron Unit, Copenhagen University Hospital Rigshospitalet, Copenhagen, Denmark*

The serotonin (5-hydroxytryptamine [5-HT]) 7 receptor (5-$HT_7$R) is the most recently discovered 5-HT receptor, and its physiologic and possible pathophysiologic roles are not fully elucidated. So far, no suitable 5-$HT_7$R PET radioligand is available, thus limiting the investigation of this receptor in the living brain. Here, we present the radiosynthesis and in vivo evaluation of Cimbi-712 (3-{4-[4-(4-methylphenyl)piperazine-1-yl]butyl}p-1,3-dihydro-2*H*-indol-2-one) and Cimbi-717 (3-{4-[4-(3-methoxyphenyl)piperazine-1-yl]butyl}-1,3-dihydro-2*H*-indol-2-one) as selective 5-$HT_7$R PET radioligands in the pig brain. The 5-$HT_7$R distribution in the postmortem pig brain is also assessed. **Methods:** In vitro autoradiography with the 5-$HT_7$R selective radioligand $^3$H-labeled (*R*)-3-(2-(2-(4-methylpiperidin-1-yl) ethyl)pyrrolidine-1-sulfonyl)phenol (SB-269970) was performed on pig brain sections to establish the 5-$HT_7$R binding distribution. Radiolabeling of 5-$HT_7$R selective compounds was performed in an automated synthesis module in which we conducted either palladium-mediated cross coupling ($^{11}$C-Cimbi-712) or conventional *O*-methylation ($^{11}$C-Cimbi-717) using $^{11}$C-MeI and $^{11}$C-MeOTf, respectively. After intravenous injection of the radioligands in Danish Landrace pigs, the in vivo brain distribution of the ligands was studied. Specific binding of $^{11}$C-Cimbi-712 and $^{11}$C-Cimbi717 to 5-$HT_7$R was investigated by intravenous administration of SB-269970 before a second PET scan. **Results:** High 5-$HT_7$R density was found in the thalamus and cortical regions of the pig brain by autoradiography. The radiosynthesis of both radioligands succeeded after optimization efforts (radiochemical yield, ~20%–30% at the end of synthesis). Time–activity curves of $^{11}$C-Cimbi-712 and $^{11}$C-Cimbi-717 showed high brain uptake and distribution according to 5-$HT_7$R distribution, but the tracer kinetics of $^{11}$C-Cimbi-717 were faster than $^{11}$C-Cimbi-712. Both radioligands were specific for 5-$HT_7$R, as binding could be blocked by pretreatment with SB-269970 for $^{11}$C-Cimbi-717 in a dose-dependent fashion. For $^{11}$C-Cimbi-717, nondisplaceable binding potentials of 6.4 ± 1.2 ($n$ = 6) were calculated in the thalamus. **Conclusion:** Both $^{11}$C-Cimbi-712 and $^{11}$C-Cimbi-717 generated a specific binding in accordance with 5-$HT_7$R distribution and are potential PET radioligands for 5-$HT_7$R. $^{11}$C-Cimbi-717 is the better candidate because of the more reversible tracer kinetics, and this radioligand showed a dose-dependent decline in cerebral binding after receptor blockade. Thus, $^{11}$C-Cimbi-717 is currently the most promising radioligand for investigation of 5-$HT_7$R binding in the living human brain.

**Key Words:** $^{11}$C-Cimbi-717; $^{11}$C-Cimbi-712; 5-$HT_7$ receptor; PET; novel radioligand

**J Nucl Med 2014; 55:640–646**
DOI: 10.2967/jnumed.113.128983

The serotonergic system plays a key modulatory role in the brain and is a target for many drug treatments for brain disorders either through reuptake blockade or interactions with one or more of the 14 subtypes of 5-hydroxytryptamine (5-HT) receptors. Our knowledge about the behavior of the 5-HT system in vivo is still scattered, and most of the understanding is derived from animal models. However, the use of imaging techniques such as positron emission tomography (PET) and the increasing number of radioligands for the 5-HT receptors enable in vivo investigation of the 5-HT system in the human brain.

The 5-$HT_7$ receptor (5-$HT_7$R) is the most recently discovered 5-HT receptor, and its biologic functions are not fully elucidated. However, its implications in brain disorders such as depression and schizophrenia (*1*) make it an interesting target for both drug discovery and radioligand development. Both pharmacologic blockade of 5-$HT_7$R and inactivation of the receptor gene led to an antidepressant-like behavioral profile in the forced swim test and in the tail suspension test (*2–5*). Pharmacologic blockade of 5-$HT_7$R also presented anxiolytic effects in animal models of anxiety (*5,6*).

Currently, no well-validated radioligand is available for in vivo imaging of 5-$HT_7$R. Interestingly, the 5-$HT_7$R and the 5-$HT_{1A}$R are the receptors for which 5-HT has the highest affinity. This is relevant for the aim of discovering a radioligand that is sensitive to changes in cerebral levels of endogenous 5-HT. If the competition model applies, the probability of measuring a signal change in response to a pharmacologic challenge that changes 5-HT levels will depend solely on the affinity of 5-HT to the target receptor (*7*).

Several potent and selective ligands for 5-$HT_7$R have been discovered, but so far only a limited number of PET radioligands have been evaluated in vivo. $^{11}$C-DR4446 had good blood–brain barrier permeability and was metabolically stable but showed only a minimal specific binding component (*8*). The 5-$HT_7$R antagonist (*R*)-3-(2-(2-(4-methylpiperidin-1-yl)ethyl)pyrrolidine-1-sulfonyl)

Received Apr. 3, 2013; revision accepted Dec. 4, 2013.
For correspondence or reprints contact: Gitte M. Knudsen, Center for Integrated Molecular Brain Imaging, Copenhagen University Hospital, Rigshospitalet, Blegdamsvej 9, DK-2100 Copenhagen, Denmark.
E-mail: gmk@nru.dk
Published online Feb. 24, 2014.

phenol (SB-269970) has been used as a lead structure for discovering $^{18}$F-labeled radioligands. $^{18}$F-1-{2-[(2*S*)-1-(phenylsulfonyl) pyrrolidin-2-yl]ethyl}piperidin-4-yl 4-fluorobenzoate and 1-(2-{(2*R*)-1-[(2-$^{18}$F-fluorophenyl)sulfonyl]pyrrolidin-2-yl}ethyl)-4-methylpiperidine ($^{18}$F-2FP3) were evaluated ex vivo in rats and in vivo in cats (*9,10*). However, no input function was obtained while evaluating $^{18}$F-2FP3. Furthermore, the 5-HT$_7$R binding distribution was not evaluated in cats, thus making it difficult to verify if the binding of $^{18}$F-2FP3 was specific to 5-HT$_7$R. We recently also reported the evaluation of a 5-HT$_7$R PET radioligand, $^{11}$C-Cimbi-806, that displayed selectivity in vitro, but the lack of blocking effect by SB-269970 in vivo led us to conclude that this compound does not selectively image the 5-HT$_7$R in vivo (*11*).

Further work with the oxindole compound class led to the synthesis of a group of compounds including Cimbi-712 (3-{4-[4-(4-methylphenyl)piperazine-1-yl]butyl}p-1,3-dihydro-2*H*-indol-2-one) and Cimbi-717 (3-{4-[4-(3-methoxyphenyl)piperazine-1-yl] butyl}-1,3-dihydro-2*H*-indol-2-one). The affinity of both Cimbi-712 and Cimbi-717 is in the lower nanomolar range for 5-HT$_7$R, with an inhibition constant ($K_i$) of 1.1 and 2.6 nM, respectively (*12*). Cimbi-712 is 2,191-fold selective for 5-HT$_7$R over 5-HT$_{1A}$R ($K_i$ for the 5-HT$_{1A}$R is 2,410 nM), whereas Cimbi-717 is 130-fold selective ($K_i$ for the 5-HT$_{1A}$R is 261 nM). From the outcome of the affinity testing on a range of receptors, Cimbi-712 displayed slightly higher selectivity for 5-HT$_7$R than did Cimbi-717 (*12*).

Here, we report the $^{11}$C-labeling and in vivo evaluation, including receptor occupancy measurements, of two novel 5-HT$_7$R selective PET radioligands in Danish Landrace pigs. For comparison between in vivo and postmortem receptor distribution, we also investigated the distribution of 5-HT$_7$R in the pig brain.

## MATERIALS AND METHODS

### In Vitro Autoradiography

One brain hemisphere of a 30-kg Danish Landrace pig was sliced on a HM500OM cryostat (Microm International GmbH) in 20-μm coronal sections except for the cerebellum, which was sliced in the sagittal plane. Sections were thaw-mounted on Superfrost Plus glass slides (Thermo Scientific) and stored at −80°C until use. Autoradiography was performed at room temperature in 50 mM Tris-HCl buffer (pH 7.4) with 5 nM $^3$H-SB-269970 (1,476.3 MBq [39.9 mCi]/μmol at synthesis [January 2012]; PerkinElmer). Nonspecific binding was determined by adding 10 μM SB-258719 (3-methyl-*N*-[(1*R*)-1-methyl-3-(4-methyl-1-piperidinyl)propyl]-*N*-methylbenzenesulfonamide hydrochloride; Tocris Bioscience). Sections were preincubated in buffer for approximately 30 min and then incubated with radioactive buffer for 2 h. Sections were then washed for 1 × 5 min and for 2 × 10 min in 50 mM Tris-HCl buffer, rinsed in distilled $H_2O$ for 20 s, and dried before exposure to tritium-sensitive plates (Fujifilm Europe GmbH) for 19 d.

Calibration, quantification, and data evaluation of all autoradiography images were done with ImageJ analysis software (http://rsb.info.nih.gov/ij/). Regions of interest were hand-drawn around anatomic landmarks—for example, borders of sections—for each brain region, and the mean pixel density was measured in each brain region as outcome. A third-degree exponential calibration function of decay-corrected $^3$H-microscales (GE Healthcare) was used to convert mean pixel density to receptor binding measured in kBq/mg tissue equivalents (TE). Finally, the decay-corrected specific activity of $^3$H-SB-269970 was used to convert kBq/mg TE to fmol/mg TE.

### Organic Synthesis

The precursors and reference compounds were synthesized as racemates as previously described (*12,13*).

### Radioligand Preparation

*$^{11}$C-Cimbi-717.* $^{11}$C-methyl trifluoromethanesulfonate, produced using a fully automated system, was transferred in a stream of helium to a 1.1-mL vial containing the labeling precursor (0.3–0.4 mg, 0.8–1.0 μmol), 0.5 M $K_2CO_3$ (14 μL, 7 μmol), and MeCN (300 μL). The resulting sealed mixture was heated at 60°C for 5 min and then separated by high-performance liquid chromatography (HPLC) on a Luna 5-μm C18(2) 100-Å column (Phenomenex Inc.) (250 × 10 mm, 50:50 acetonitrile:0.01 M sodium borate buffer, at a flow rate of 6 mL/min). Retention times were 610 s for $^{11}$C-Cimbi-717 and 300 s for the precursor. The fraction corresponding to the labeled product was collected in sterile water (150 mL), and the resulting solution was passed through a solid-phase C18 Sep-Pak extraction column (Waters Corp.), which had been preconditioned with ethanol (10 mL), followed by isotonic sodium chloride solution (20 mL). The column was flushed with sterile water (3 mL). Then, the trapped radioactivity was eluted through a sterile filter with ethanol (3 mL), followed by isotonic sodium chloride solution (3 mL), into a 20-mL vial containing sodium phosphate–buffered saline (9 mL, 100 mM, pH 7), giving a 15-mL solution of racemic $^{11}$C-Cimbi-717 with a pH of approximately 7.

*$^{11}$C-Cimbi-712.* $^{11}$C-Cimbi-712 was produced as described previously (*13*). The HPLC fraction corresponding to the labeled product was collected in sterile water (150 mL), and the resulting solution was passed through a solid-phase C18 Sep-Pak extraction column, which had been preconditioned with ethanol (10 mL), followed by water (20 mL). The trapped radioactivity was eluted through a sterile filter with ethanol (3 mL) into a 20-mL vial containing sodium phosphate–buffered saline (9 mL, 100 mM, pH ~7), giving a 12-mL solution of racemic $^{11}$C-Cimbi-712 with a pH of approximately 7.

### Determination of Radiochemical Purity and Specific Radioactivity

Chemical and radiochemical purities were assessed on the same sample by HPLC analysis. Specific activity of the radioligands was calculated from 3 consecutive HPLC analyses (average) and determined by comparing the area of the ultraviolet absorbance peak corresponding to the radiolabeled product on the HPLC chromatogram with a standard curve relating mass to ultraviolet absorbance (λ = 225 nm). $^{11}$C-Cimbi-712 and $^{11}$C-Cimbi-717 were analyzed with HPLC using a Luna 5-μm C18(2) 100-Å column (150 × 4.6 mm, 50:50 MeCN:0.01 M borax buffer, at a flow rate of 2 mL/min). Retention times were 180 s for $^{11}$C-Cimbi-717 and 290 s for $^{11}$C-Cimbi-712).

### Animal Procedure

Eight female Danish Landrace pigs (mean weight ± SD, 19 ± 2.0 kg) were used for in vivo PET imaging. All animal procedures were approved by the Danish Council for Animal Ethics (journal no. 2012-15-2934-00156).

### PET Protocol

$^{11}$C-Cimbi-712 was given as an intravenous bolus injection over 20 s, and the injected doses were 155 and 110 MBq for baseline scans ($n$ = 2) and 123 and 73 MBq for scans for which SB-269970 was preadministered ($n$ = 2). $^{11}$C-Cimbi-717 was also given as an intravenous bolus over 20 s, and the injected dose (mean ± SD) was 236 ± 117 MBq for baseline scans ($n$ = 6; range, 115–435 MBq) and 147 ± 82.1 MBq for scans for which a preblocking agent was administered ($n$ = 6; range, 40–277 MBq). The pigs were subsequently scanned for 90 min in list mode with a high-resolution research tomograph (HRRT; Siemens AG), with scanning starting at the time of injection (0 min). Immediately after the baseline scan (90 min), SB-269970 (Tocris Bioscience), a selective 5-HT$_7$R antagonist (*14*), was given intravenously as a bolus infusion (0.2, 1.0, or 4.2 mg/kg/h), and rescanning started after 30 min of pretreatment with SB-269970. In one pig, a 0.5 mg/kg dose of prazosin (Sigma Aldrich), an $\alpha_1$ adren-

ergic receptor antagonist (*15,16*), was given as an intravenous infusion before injection of $^{11}$C-Cimbi-717.

### Whole-Blood and Plasma Input Functions

During the first 30 min of the scans, radioactivity in arterial whole blood was continuously measured using an ABSS autosampler (Allogg Technology) counting coincidences in a lead-shielded detector. Concurrently, arterial whole blood was sampled manually at 2.5, 5, 10, 20, 30, 40, 50, 70, and 90 min after injection and radioactivity was measured in whole blood and plasma using a well counter (Cobra 5003; PerkinElmer). Cross calibration between the HRRT scanner, the autosampler, and the well counter allowed for the determination of plasma input functions.

### Metabolite Analysis

Radiolabeled parent compound and metabolites were measured in plasma using HPLC with online radioactivity detection. In short, $^{11}$C-Cimbi-712 and $^{11}$C-Cimbi-717 were separated from their respective radiolabeled metabolites by direct injection of plasma in a column-switching HPLC system. Whole-blood samples were centrifuged (3,500 rpm, 7 min), and the supernatant plasma fraction was collected and filtered through a 0.45-μM syringe filter before analysis with online radioactive detection, as previously described (*17,18*).

### Determination of Free Fraction

The free fraction of $^{11}$C-Cimbi-717 in pig plasma was measured using an equilibrium dialysis method as previously described (*19*) and calculated as the ratio between radioactivity in a buffer and plasma compartment after equilibrium between the chambers had been reached after 3 h.

### Quantification of PET Data

Ninety-minute list-mode PET data were reconstructed into 38 dynamic frames of increasing length (6 × 10, 6 × 20, 4 × 30, 9 × 60, 2 × 180, 8 × 300, and 3 × 600 s). Images consisted of 207 planes of 256 × 256 voxels of 1.22 × 1.22 × 1.22 mm. A summed picture of all counts in the 90-min scan was reconstructed for each pig and used for coregistration to a standardized MR imaging–based atlas of the Danish Landrace pig brain, similar to that previously published (*18,19*). The time–activity curves were calculated for the following volumes of interest: cerebellum, cortex, hippocampus, lateral and medial thalamus, caudate nucleus, and putamen. The activity in the striatum is defined as the mean radioactivity in the caudate nucleus and putamen. The activity in the thalamus is calculated as the mean radioactivity in the lateral and medial thalamus. Radioactivity in all volumes of interest was calculated as the average of radioactive concentration (Bq/mL) in the left and right sides. The outcome measure in the time–activity curves was calculated as radioactive concentration in the volume of interest (in kBq/mL) normalized to the injected dose corrected for animal weight (in kBq/kg), yielding standardized uptake values (g/mL).

Distribution volumes ($V_T$) for the volumes of interest were calculated on the basis of 3 different models: the 1-tissue-compartment (1-TC), 2-tissue-compartment (2-TC), and Logan linearization models. A single parent fraction curve fitted to a biexponential function, obtained from the average across all scans in the study, was used to generate individual metabolite-corrected plasma concentration curves. The $V_T$ of baseline and blocked conditions was used to determine the nondisplaceable distribution volume ($V_{ND}$) by use of the Lassen plot and thereby allow for calculation of the nondisplaceable binding potential $BP_{ND}$ (*20*). All modeling was initiated with the same starting parameters, and SD coefficient variance was below 15% for macroparameters (the rate constant $K_1$ and $V_T$). Datasets that did not fulfill this criterion were not included in the results. Of the 176 fittings for $^{11}$C-Cimbi-717, 2 failed for the 1-TC, 31 failed for the 2-TC, and 7 failed for the Logan linearization model. Of the 40 attempts for $^{11}$C-Cimbi-712, 2 failed for the 1-TC, 12 failed for the 2-TC, and 11 failed for the Logan linearization model.

## RESULTS

### 5-HT$_7$R Distribution in the Pig Brain

The highest $^3$H-SB-269970 binding was found in small subregions of the thalamus (62.2 fmol/mg TE), amygdala (48.3 fmol/mg TE), and cingulate cortex (44.9 fmol/mg TE) (Table 1; Fig. 1). Low binding was found in the striatum and especially in the cerebellum (13.4 fmol/mg TE). In the cortical regions, binding increased toward the posterior parts of the pig brain, with the highest cortical binding found in the cingulate lobe (Supplemental Fig. 1; supplemental materials are available at http://jnm.snmjournals.org).

### Radiochemistry

Radiolabeling of $^{11}$C-Cimbi-712 has previously been described (*13*). In brief, $^{11}$C-Cimbi-712 was labeled with a radiochemical yield (RCY) of 0.3–0.5 GBq and with a specific activity of 106 ± 68 GBq/μmol ($n$ = 4) in a total synthesis time of 40–50 min.

Radiolabeling of $^{11}$C-Cimbi-717 underwent extensive optimization (Supplemental Table 1) as compared with $^{11}$C-Cimbi-712 (*13*), now using 0.3 mg of precursor, 14 μL of 0.5 M $K_2CO_3$ (1 equivalent), and $^{11}$C-$CH_3$OTf on a fully automated system (decay-corrected RCY, ~20%) (Fig. 2). Two major radioactive peaks were detected. The minor peak corresponded to $^{11}$C-Cimbi-717 (~600 s) (further information is in the supplemental materials). The precursor eluted approximately 300 s before the radiolabeled product as indicated by the ultraviolet-absorption chromatogram (Supplemental Fig. 2). The radiosynthesis, including HPLC purification and formulation, generated an injectable solution of $^{11}$C-Cimbi-717 (radiochemical purity > 97%, chemical purity > 98%) within 40–50 min. Typically, 0.2–0.4 GBq of $^{11}$C-Cimbi-717 were

**TABLE 1**
5-HT$_7$R Distribution in Different Brain Regions Determined by $^3$H-SB-269970 Autoradiography

| Region | Specific binding (fmol/mg TE) | Number of sections in region |
|---|---|---|
| Cortical regions | | |
| Prefrontal | 32.7 ± 1.60 | 2 |
| Frontal | 38.3 ± 2.68 | 5 |
| Temporal | 41.0 ± 3.03 | 7 |
| Cingulate | 44.9 ± 2.60 | 16 |
| Occipital | 33.2 ± 2.40 | 4 |
| Striatum | | |
| Putamen | 21.6 ± 1.64 | 5 |
| Caudate | 24.4 ± 2.81 | 5 |
| Thalamus | 45.6 ± 0.19 | 3 |
| Thalamus (high-binding subregion) | 62.0 ± 5.53 | 2 |
| Hypothalamus | 43.0 ± 6.03 | 3 |
| Hippocampus | 37.5 ± 3.35 | 6 |
| Amygdala | 48.3 ± 5.01 | 4 |
| Cerebellum | 13.4 ± 2.22 | 2 |

5-HT$_7$R distribution is determined as specific binding of 5 nM $^3$H-SB-269970 in fmol/mg TE. Values are given as mean ± SD. Mean is for 3 independent experiments.

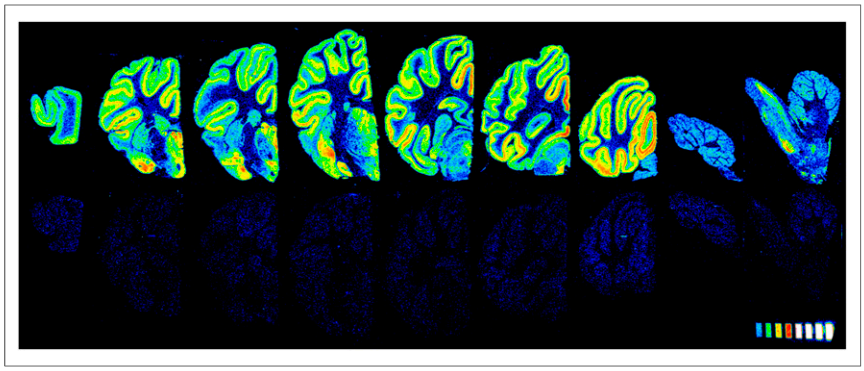

**FIGURE 1.** Representative sections of 5-$HT_7$R autoradiography. Sections were incubated with 5 nM $^3$H-SB-269970 to determine total binding (upper row) and with 10 μM SB-258719 to determine nonspecific binding (lower row).

isolated, with a specific activity of 69.7 ± 41.0 GBq/μmol ($n$ = 12) at the end of synthesis. No precursor could be detected in the final formulation.

### In Vivo Distribution

With $^{11}$C-Cimbi-712, the highest brain uptake was observed in the thalamus and the lowest uptake in the cerebellum. Time–activity curves displayed slow kinetics, with peak uptake after approximately 50 min (Fig. 3A). Pretreatment of the animals with 1.0 mg/kg/h SB-269970 decreased binding by approximately 50% in all regions. Like $^{11}$C-Cimbi-712, $^{11}$C-Cimbi-717 showed the highest brain uptake in the thalamus and the lowest uptake in the cerebellum (Fig. 3D). The $^{11}$C-Cimbi-717 time–activity curves indicated reversible binding in the pig brain, with fast brain uptake and a more pronounced decline in tissue time–activity curves than was found for $^{11}$C-Cimbi-712 (Fig. 3B). Pretreatment of the animal with SB-269970 (1.0 mg/kg/h and 4.2 mg/kg/h) decreased $^{11}$C-Cimbi-717 uptake and increased the rate of washout in all brain regions.

Because no significant changes were observed between the baseline and blocking experiments in the composition of parent compound and other metabolites over the time course of the scan (data not shown), a single parent fraction obtained from the average over all scans with $^{11}$C-Cimbi-717 was computed and used to generate arterial plasma input time–activity curves. No changes in arterial input function were observed between the baseline and blocking experiments. Receptor binding of $^{11}$C-Cimbi-717 quantified with the 1-TC model showed the $V_T$ to be highest in the thalamus (16 ± 2.5 mL/cm$^3$) and lowest in the cerebellum (6.6 ± 1.2 mL/cm$^3$), indicating good regional separation, as also confirmed by the time–activity curves (Fig. 3B). $V_T$ was also calculated for all doses of SB-269970 and prazosin (Fig. 4C). A dose-dependent reduction in $V_T$ was observed with SB-269970, with significant reductions with the doses 1.0 mg/kg/h ($P < 0.01$) and 4.2 mg/kg/h ($P < 0.001$) in all regions except the cerebellum. The slope of the occupancy curve for prazosin was not significantly different from 0, supporting the likelihood that prazosin does not alter the binding of $^{11}$C-Cimbi-717 in vivo.

Receptor binding of $^{11}$C-Cimbi-712 was quantified with the 1-TC model. $V_T$s were—as with $^{11}$C-Cimbi-717—highest in the thalamus (87.5 and 54.9 mL/cm$^3$) and lowest in the cerebellum (35.2 and 32.1 mL/cm$^3$). The $V_T$s of the pretreated scans revealed a decrease in binding, although the decrease could not be reliably statistically assessed (Fig. 4A). The occupancy slopes were, however, significantly different from 0, verifying that SB-269970 did block the binding of $^{11}$C-Cimbi-712.

Based on occupancy plots of $^{11}$C-Cimbi-717 (Fig. 4D), the $V_{ND}$ and occupancy were extracted from the linear regression. The $^{11}$C-Cimbi-717 $V_{ND}$ was on average 2.1 ± 0.8 mL/cm$^3$ (mean ± SD, $n$ = 5), and intravenous pretreatment with 0.2 mg/kg/h SB-269970 resulted in 25.4% occupancy, whereas pretreatment with the higher doses of 1.0 and 4.2 mg/kg/h resulted in 59.9% and 75.4% occupancy, respectively. Consequently, the $BP_{ND}$ of $^{11}$C-Cimbi-717 at baseline in the thalamus and cerebellum were calculated to be 6.4 ± 1.2 and 2.1 ± 0.6 ($n$ = 6), respectively.

Treatment with 1.0 mg/kg/h SB-269970 before $^{11}$C-Cimbi-712 injection resulted in an occupancy of 75.3% and a $V_{ND}$ of 8.57 mL/cm$^3$ (Fig. 4B). Consequently, the $BP_{ND}$ of $^{11}$C-Cimbi-712 in the thalamus is 7.3 based on average $V_T$s and $V_{ND}$s.

Comparison of the in vitro and in vivo binding data revealed significant positive correlations between $^3$H-SB-269970 binding in vitro and $^{11}$C-Cimbi-712 ($P$ = 0.016) and $^{11}$C-Cimbi-717 ($P < 0.001$) binding in vivo (Fig. 5).

The free fraction of $^{11}$C-Cimbi-717 in plasma was on average 6.7% at equilibrium.

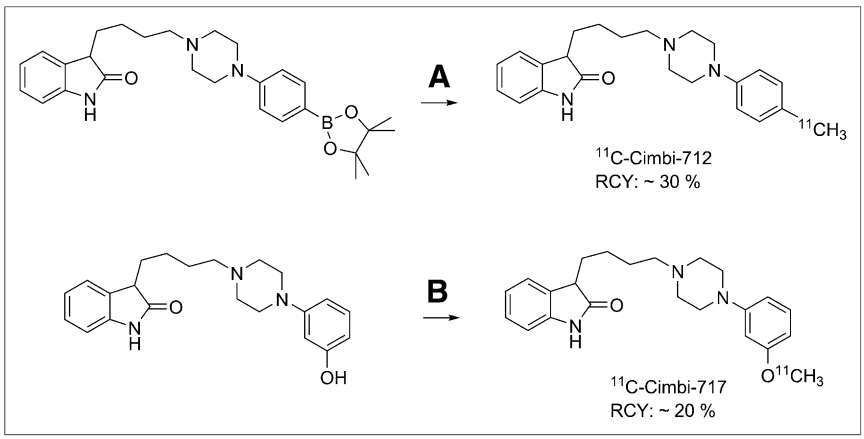


**FIGURE 2.** Radiosyntheses of $^{11}$C-Cimbi-712 and $^{11}$C-Cimbi-717. Reagents and conditions: $^{11}$C-$CH_3$I, $K_2CO_3$, $Pd_2(dba)_3$, P(o-tolyl)$_3$, 60°C, DMF:$H_2O$ (v:v 9:1) (A) and $^{11}$C-$CH_3$OTf, 0.3 mg precursor, MeCN, $K_2CO_3$ (1 equivalent), 60°C, 5 min (B).

### Metabolism

Radio-HPLC analysis of pig plasma revealed that after intravenous injection, $^{11}$C-Cimbi-717 was relatively slowly metabolized (50% remaining after 30 min), and two radiometabolites were observed (Fig. 6). The polar metabolite fraction increased during the 90-min scanning time. The other more lipophilic metabolite was detected in relatively low amounts (~15%). However, this metabolite was less lipophilic than $^{11}$C-Cimbi-717.

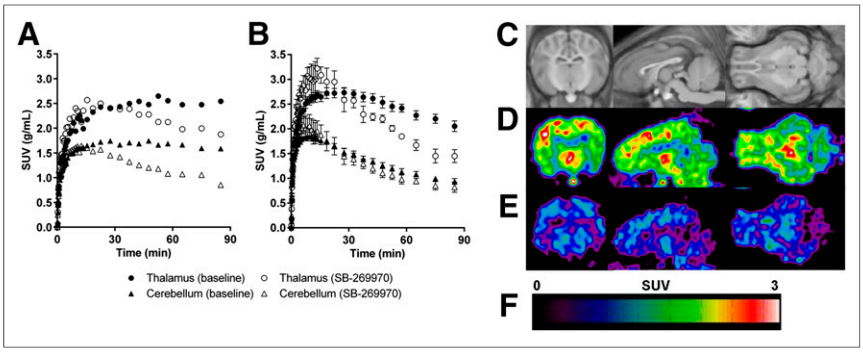


**FIGURE 3.** (A) Time–activity curves for $^{11}$C-Cimbi-712 at baseline (● and ▲, $n = 2$) and after blocking with 1.0 mg/kg/h SB-269970 (○ and △, $n = 2$). (B) Time–activity curves for $^{11}$C-Cimbi-717 at baseline (● and ▲, $n = 6$) and after blocking with 1.0 mg/kg/h SB-269970 (○ and △, $n = 3$). (C) MR-based atlas of pig brain. (D) $^{11}$C-Cimbi-717 baseline summed PET images from 0 to 90 min. (E) SB-269970–pretreated $^{11}$C-Cimbi-717 summed PET images from 0 to 90 min. (F) Color bar of standardized uptake value (SUV) (g/mL). Error bars = SEM.

## DISCUSSION

Here we have presented the radiosyntheses and in vivo evaluation of two novel 5-HT$_7$R radioligands, $^{11}$C-Cimbi-712 and $^{11}$C-Cimbi-717. To enable comparisons between in vitro and in vivo data, we have also assessed for the first time the cerebral 5-HT$_7$R distribution in the pig brain.

Consistent with observations in the human brain (*21,22*) and brain membrane binding assays in different species (*23*), in vitro data with $^3$H-SB-269970 showed that 5-HT$_7$R distribution in the pig brain was fairly homogeneous in the neocortex but differed more across the remaining brain regions. Our data also showed that the hypothalamus, thalamus, and amygdala are areas with high 5-HT$_7$R density, as is in line with the involvement of 5-HT$_7$R in circadian rhythm controlled by the suprachiasmatic nucleus (*24,25*). As described for human brain tissue, $^3$H-SB-269970 binding in the pig striatum was low. We found low 5-HT$_7$R binding in the pig cerebellum, corresponding to a study showing low amounts of 5-HT$_7$R messenger RNA in cerebellum in pigs (*26*). We found a general high binding in the cerebral cortex of the pig brain as reported earlier for membrane binding assays (*23*). Although the cortical binding pattern did not resemble that of 5-HT$_{2A}$R or 5-HT$_{1A}$R (*27*), we confirmed the specificity of $^3$H-SB-269970 through autoradiographic blocking experiments with the specific 5-HT$_{1A}$R and 5-HT$_{2A}$R antagonists WAY-100635 and MDL-100907 (data not shown). No displacement was found with WAY-100635, but in accordance with the affinity of MDL-100907 ($K_i \sim 50$ nM) toward 5-HT$_7$R (*28*), a 40% displacement was observed.

Although $^{11}$C-Cimbi-717 was successfully labeled in sufficient RCY for the PET experiments, we did not succeed in further optimizing the RCY. We speculate that the major radioactive side product is due to methylation of the oxindole moiety, and if so, the introduction of a protecting group at the N-1 position of the oxindole may reduce the formation of the observed side product. Although the racemic material could be separated on chirale HPLC, the stereogenic center epimerizes rapidly. Thus, all compounds in this study have been investigated as the racemate. The quantification is therefore an average of binding of two enantiomers, and it is possible that one of the enantiomers is superior to the other.

In vivo evaluation of $^{11}$C-Cimbi-717 demonstrated a high brain uptake and a binding distribution similar to that of 5-HT$_7$R found in vitro; thalamus has the highest and cerebellum the lowest $V_T$, consistent with the $^3$H-SB-269970 autoradiography. $^{11}$C-Cimbi-717 binding in the striatum was not quite in line with the correlation between in vivo binding in other regions and in vitro autoradiography binding. Further analysis of these differences revealed that this discrepancy between 5-HT$_7$R binding in vivo and in vitro was larger for the putamen than for the caudate nucleus; thus, the discrepancy could be due to binding to an unknown target, for which either of the enantiomers of $^{11}$C-Cimbi-717 has affinity. However, the occupancy plot did not reveal lower displacement in the striatal regions. We suspect

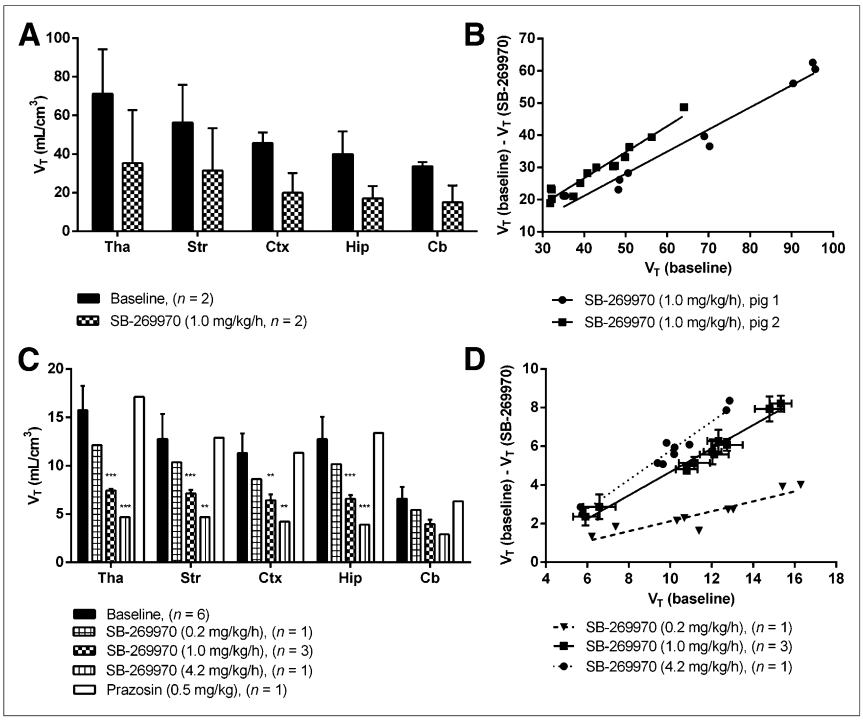


**FIGURE 4.** (A) $V_T$s for $^{11}$C-Cimbi-712 quantified by 1-TC modeling. (B) Occupancy plots for $^{11}$C-Cimbi-712, where $V_T$s for individual pigs are shown. (C) $V_T$s for $^{11}$C-Cimbi-717 quantified by 1-TC modeling. (D) Occupancy plots for $^{11}$C-Cimbi-717 with 3 different doses of SB-269970. In A and C, bars represent mean ± SD; in B and D, bars represent mean ± SEM. $^{**}P < 0.01$ and $^{***}P < 0.001$ in comparison to baseline data within each volume of interest on statistical analysis with 2-way ANOVA and Bonferroni posttest. Tha = thalamus; Str = striatum; Ctx = cortex; Hip = hippocampus; Cb = cerebellum.

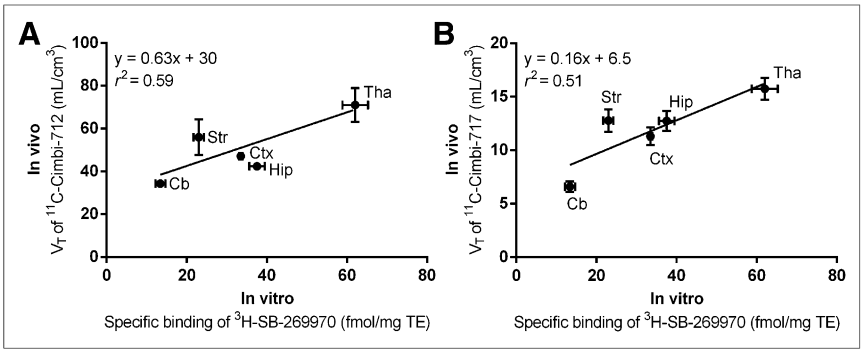


**FIGURE 5.** Comparison of 5-HT$_7$R brain distribution determined by $^3$H-SB-269970 autoradiography and by in vivo PET experiments using baseline $V_T$s of $^{11}$C-Cimbi-712 ($n$ = 2) (A) and $^{11}$C-Cimbi-717 ($n$ = 6) (B). Cb = cerebellum; Ctx = cortex; Hip = hippocampus; Str = striatum; Tha = thalamus. Error bars represent mean ± SEM.

that the difference observed between the in vitro and in vivo results are due to inhomogeneity in the autoradiography experiments. With autoradiography, only a few cross sections were evaluated, whereas in PET, binding in the whole region is evaluated. The putamen is near the amygdala in the pig brain, and partial-volume effects may affect the signal from this high-binding region, leading to an overestimation of the $^{11}$C-Cimbi-712 and $^{11}$C-Cimbi-717 binding in the putamen. The correlation between in vitro and in vivo binding was not as strong for $^{11}$C-Cimbi-712 as for $^{11}$C-Cimbi-717. Along with the difference in binding in the striatum, $^{11}$C-Cimbi-712 also displayed equal uptake in the hippocampus and cerebellum, a finding that is not in line with what we see with $^3$H-SB-269970 autoradiography. This discrepancy in binding between $^{11}$C-Cimbi-712 and $^{11}$C-Cimbi-717 in the hippocampus could be due to off-target binding. Highest binding is, however, still observed in the thalamus, consistent with the autoradiography results.

Pretreatment with SB-269970 resulted in a dose-dependent decrease in $^{11}$C-Cimbi-717 binding in the pig brain supporting 5-HT$_7$R selectivity in vivo for $^{11}$C-Cimbi-717. $V_T$ decreased in all regions examined, including the cerebellum. Although this decrease in binding in the cerebellum was not statistically significant, it confirms the in vitro autoradiography data and the literature data that have found 5-HT$_7$R to be present in the cerebellum (*26*). This decrease in binding in the cerebellum also invalidates the cerebellum as a reference region for a reference tissue model analysis of the PET data. In the absence of a reference region, we determined the nondisplaceable binding using the occupancy plot. Because of the affinity of Cimbi-717 for the $\alpha_1$ adrenergic receptor ($K_i$ = 47 nM) (*12*), we ensured that pretreatment with prazosin, an $\alpha_1$ adrenergic receptor antagonist, did not result in any significant decrease in $^{11}$C-Cimbi-717 $V_T$. $^{11}$C-Cimbi-712 binding was blocked with SB-269970, supporting the possibility that this radioligand also labels 5-HT$_7$R specifically. The slow kinetics of $^{11}$C-Cimbi-712, however, complicate modeling of the binding, resulting in large variations in the outcome measures ($V_T$) and consequently also larger uncertainties in the calculated occupancy and $V_{ND}$.

The average nonspecific binding in the pig brain, $V_{ND}$, of $^{11}$C-Cimbi-717 as determined by the occupancy plot was 2.1 mL/cm$^3$ and thus comprised about 15% of the $V_T$ in the high-binding regions. This ratio of specific-to-nonspecific binding is larger than what is obtained by other PET ligands evaluated in the same species, for example, approximately 50% for $^{11}$C-NS14492 and approximately 35% for $^{11}$C-SB2047145 (*19,29*).

Modeling of the $^{11}$C-Cimbi-717 data was done with the 1-TC model first because of the simplicity of the model, second because more regions converged with this model compared with 2-TC, and finally because the Akaike information criterion was generally lower for the 1-TC than for the 2-TC (Supplemental Table 2). The Logan linearization model underestimated the $V_T$ values by 10%–15% compared with both the 1-TC and the 2-TC.

The systemic metabolism of $^{11}$C-Cimbi-717 was relatively slow compared with other radioligands evaluated in pigs (*11,18,19*), with approximately 60% of the total plasma activity arising from the parent compound left after 20 min. Metabolism was nonsignificantly faster after blockade with SB-269970, as could be explained by an increased availability in the blood and thus an increased availability to enzymatic degradation. No effects on metabolism were observed with prazosin.

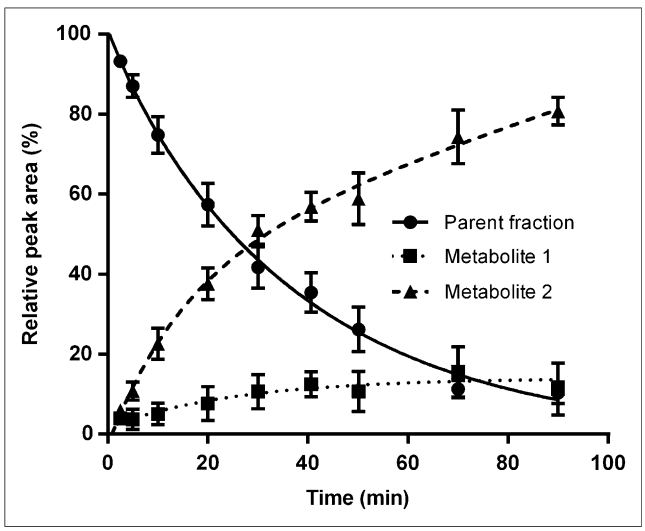


**FIGURE 6.** Metabolism of $^{11}$C-Cimbi-717. Three radioactive compounds could be detected with radio-HPLC: $^{11}$C-Cimbi-717 (parent compound) and two radiolabeled metabolites, both of which had lower retention time than parent compound. Data are presented as mean ± SEM.

## CONCLUSION

$^{11}$C-Cimbi-712 and $^{11}$C-Cimbi-717 were both successfully radiolabeled in sufficient RCYs for in vivo evaluation in the pig. Of the two novel radioligands for brain imaging of 5-HT$_7$R, $^{11}$C-Cimbi-717 generated the highest brain uptake and showed more reversible tracer kinetics than $^{11}$C-Cimbi-712—benefits that are important for quantification. Both $^{11}$C-Cimbi-712 and $^{11}$C-Cimbi-717 had a regional distribution pattern compatible with 5-HT$_7$R distribution in the pig brain, as assessed independently by autoradiography. Finally, $^{11}$C-Cimbi-717 showed a dose-dependent decrease in binding after pretreatment with the 5-HT$_7$R–specific antagonist SB-269970. We conclude, on the basis of these preclinical data, that $^{11}$C-Cimbi-717 may be a useful radioligand for in vivo imaging of 5-HT$_7$R binding sites in the human brain.

## DISCLOSURE

The costs of publication of this article were defrayed in part by the payment of page charges. Therefore, and solely to indicate this fact, this article is hereby marked "advertisement" in accordance with 18 USC section 1734. Financial support by the Intra European Fellowship (MC-IEF-275329), the Faculty of Health at the University of Copenhagen, and particularly the Lundbeck Foundation is gratefully acknowledged. The John and Birthe Meyer Foundation and the Toyota Foundation are acknowledged for financial support for the HRRT scanner and HPLC system, respectively. No other potential conflict of interest relevant to this article was reported.

## ACKNOWLEDGMENTS

We thank the staff at the PET and Cyclotron Units for expert technical assistance. We also thank Mette Værum Olesen for excellent technical assistance with animal preparation.

## REFERENCES

1. Matthys A, Haegeman G, Van Craenenbroeck K, Vanhoenacker P. Role of the 5-$HT_7$ receptor in the central nervous system: from current status to future perspectives. *Mol Neurobiol.* 2011;43:228–253.
2. Bonaventure P, Kelly L, Aluisio L, et al. Selective blockade of 5-hydroxytryptamine (5-HT)7 receptors enhances 5-HT transmission, antidepressant-like behavior, and rapid eye movement sleep suppression induced by citalopram in rodents. *J Pharmacol Exp Ther.* 2007;321:690–698.
3. Guscott M, Bristow LJ, Hadingham K, et al. Genetic knockout and pharmacological blockade studies of the 5-$HT_7$ receptor suggest therapeutic potential in depression. *Neuropharmacology.* 2005;48:492–502.
4. Hedlund PB, Huitron-Resendiz S, Henriksen SJ, Sutcliffe JG. 5-$HT_7$ receptor inhibition and inactivation induce antidepressantlike behavior and sleep pattern. *Biol Psychiatry.* 2005;58:831–837.
5. Wesołowska A, Nikiforuk A, Stachowicz K, Tatarczynska E. Effect of the selective 5-$HT_7$ receptor antagonist SB 269970 in animal models of anxiety and depression. *Neuropharmacology.* 2006;51:578–586.
6. Volk B, Barkoczy J, Hegedus E, et al. (Phenylpiperazinyl-butyl)oxindoles as selective 5-$HT_7$ receptor antagonists. *J Med Chem.* 2008;51:2522–2532.
7. Paterson LM, Tyacke RJ, Nutt DJ, Knudsen GM. Measuring endogenous 5-HT release by emission tomography: promises and pitfalls. *J Cereb Blood Flow Metab.* 2010;30:1682–1706.
8. Zhang M-R, Haradahira T, Maeda J, et al. Synthesis and preliminary PET study of the 5-HT7 receptor antagonist [$^{11}$C]DR4446. *J Labelled Comp Radiopharm.* 2002;45:857–866.
9. Andriès J, Lemoine L, Mouchel-Blaisot A, et al. Looking for a 5-$HT_7$ radiotracer for positron emission tomography. *Bioorg Med Chem Lett.* 2010;20:3730–3733.
10. Lemoine L, Andries J, Le Bars D, Billard T, Zimmer L. Comparison of 4 radiolabeled antagonists for serotonin 5-$HT_7$ receptor neuroimaging: toward the first PET radiotracer. *J Nucl Med.* 2011;52:1811–1818.
11. Herth MM, Hansen HD, Ettrup A, et al. Synthesis and evaluation of [$^{11}$C]Cimbi-806 as a potential PET ligand for 5-HT(7) receptor imaging. *Bioorg Med Chem.* 2012;20:4574–4581.
12. Herth MM, Volk B, Pallagi K, et al. Synthesis and in vitro evaluation of oxindole derivatives as potential radioligands for 5-HT(7) receptor imaging with PET. *ACS Chem Neurosci.* 2012;3:1002–1007.
13. Andersen VL, Herth MM, Lehel S, Knudsen GM, Kristensen JL. Palladium-mediated conversion of para-aminoarylboronic esters into para-aminoaryl-$^{11}$C-methanes. *Tetrahedron Lett.* 2013;54:213–216.
14. Lovell PJ, Bromidge SM, Dabbs S, et al. A novel, potent, and selective 5-HT(7) antagonist: (R)-3-(2-(2-(4-methylpiperidin-1-yl)ethyl)pyrrolidine-1-sulfonyl) phenol (SB-269970). *J Med Chem.* 2000;43:342–345.
15. Cavero I, Roach AG. The pharmacology of prazosin, a novel antihypertensive agent. *Life Sci.* 1980;27:1525–1540.
16. Schwinn DA, Johnston GI, Page SO, et al. Cloning and pharmacological characterization of human alpha-1 adrenergic receptors: sequence corrections and direct comparison with other species homologues. *J Pharmacol Exp Ther.* 1995;272:134–142.
17. Gillings N. A restricted access material for rapid analysis of [$^{11}$C]-labeled radiopharmaceuticals and their metabolites in plasma. *Nucl Med Biol.* 2009;36:961–965.
18. Ettrup A, Palner M, Gillings N, et al. Radiosynthesis and evaluation of $^{11}$C-CIMBI-5 as a 5-$HT_{2A}$ receptor agonist radioligand for PET. *J Nucl Med.* 2010;51:1763–1770.
19. Kornum BR, Lind NM, Gillings N, Marner L, Andersen F, Knudsen GM. Evaluation of the novel 5-$HT_4$ receptor PET ligand [$^{11}$C]SB207145 in the Gottingen minipig. *J Cereb Blood Flow Metab.* 2009;29:186–196.
20. Cunningham VJ, Rabiner EA, Slifstein M, Laruelle M, Gunn RN. Measuring drug occupancy in the absence of a reference region: the Lassen plot re-visited. *J Cereb Blood Flow Metab.* 2010;30:46–50.
21. Hagan JJ, Price GW, Jeffrey P, et al. Characterization of SB-269970-A, a selective 5-HT(7) receptor antagonist. *Br J Pharmacol.* 2000;130:539–548.
22. Varnäs K, Thomas DR, Tupala E, Tiihonen J, Hall H. Distribution of 5-$HT_7$ receptors in the human brain: a preliminary autoradiographic study using [$^3$H] SB-269970. *Neurosci Lett.* 2004;367:313–316.
23. Thomas DR, Atkinson PJ, Hastie PG, Roberts JC, Middlemiss DN, Price GW. [$^3$H]-SB-269970 radiolabels 5-$HT_7$ receptors in rodent, pig and primate brain tissues. *Neuropharmacology.* 2002;42:74–81.
24. Lovenberg TW, Baron BM, de Lecea L, et al. A novel adenylyl cyclase-activating serotonin receptor (5-$HT_7$) implicated in the regulation of mammalian circadian rhythms. *Neuron.* 1993;11:449–458.
25. Sprouse J, Li X, Stock J, McNeish J, Reynolds L. Circadian rhythm phenotype of 5-$HT_7$ receptor knockout mice: 5-HT and 8-OH-DPAT-induced phase advances of SCN neuronal firing. *J Biol Rhythms.* 2005;20:122–131.
26. Bhalla P, Saxena PR, Sharma HS. Molecular cloning and tissue distribution of mRNA encoding porcine 5-$HT_7$ receptor and its comparison with the structure of other species. *Mol Cell Biochem.* 2002;238:81–88.
27. Ettrup A, Kornum BR, Weikop P, Knudsen GM. An approach for serotonin depletion in pigs: effects on serotonin receptor binding. *Synapse.* 2011;65: 136–145.
28. Roth BL, Craigo SC, Choudhary MS, et al. Binding of typical and atypical antipsychotic agents to 5-hydroxytryptamine-6 and 5-hydroxytryptamine-7 receptors. *J Pharmacol Exp Ther.* 1994;268:1403–1410.
29. Ettrup A, Mikkelsen JD, Lehel S, et al. $^{11}$C-NS14492 as a novel PET radioligand for imaging cerebral alpha7 nicotinic acetylcholine receptors: in vivo evaluation and drug occupancy measurements. *J Nucl Med.* 2011;52:1449–1456.